NATIONAL ADVISORY COMMITTEE FOR AERONAUTICS

TECHNICAL NOTE 3909

VERTICAL FORCE-DEFLECTION CHARACTERISTICS OF A PAIR OF 56-INCH-DIAMETER AIRCRAFT TIRES FROM STATIC AND DROP TESTS WITH AND WITHOUT PREROTATION

By Robert F. Smiley and Walter B. Horne

Langley Aeronautical Laboratory
Langley Field, Va.

Washington
February 1957

NATIONAL ADVISORY COMMITTEE FOR AERONAUTICS

TECHNICAL NOTE 3909

VERTICAL FORCE-DEFLECTION CHARACTERISTICS OF A PAIR OF 56-INCH-DIAMETER AIRCRAFT TIRES FROM STATIC AND DROP TESTS WITH AND WITHOUT PREROTATION

By Robert F. Smiley and Walter B. Horne

SUMMARY

An investigation was made to obtain information on the vertical force-deflection characteristics of a pair of 56-inch-diameter type I (smooth contour) aircraft tires under three conditions: static tests, drop tests without prerotation, and drop tests with prerotation up to 470 revolutions per minute. The experimental results together with a few simplified theoretical considerations indicated that a small but noticeable difference between the tire vertical force-deflection characteristics existed for these three conditions and that there might be similar differences between these characteristics and those for realistic landing conditions with finite horizontal velocity. Generally speaking, for increasing force, the tires are found to be least stiff for static tests, almost the same as for the static case for prerotation drop tests as long as the tires remain rotating, and appreciably stiffer for drop tests without prerotation.

The effects of the following factors on the tire force-deflection characteristics are also discussed: nature of the tire air-compression process, tire hysteresis, tire centrifugal forces, and drag loads.

INTRODUCTION

During an actual airplane landing, the relationships between the vertical ground force acting on the airplane tires and the tire vertical deflections are influenced by the rapidly varying vertical, drag, side, and rotational forces and motions which are experienced by the tires. Since the tire vertical force-deflection characteristics are essential for any study of the variation and magnitude of aircraft landing loads, some knowledge of the effects of these various forces and motions on the vertical force-deflection characteristics is desirable. The vertical force-deflection tire data which are now generally available have been obtained primarily from static tests and drop tests on nonrotating tires. Inasmuch as tests of this nature do not necessarily realistically reproduce the

force and motion variations which a tire experiences during actual landings, there is some question as to the extent that the available data can be used to provide reliable predictions of tire vertical force-deflection characteristics for realistic landing conditions.

The present investigation was undertaken in order to obtain a better insight into the factors which influence the vertical force-deflection characteristics of aircraft tires. Three types of tests were performed in the Langley drop-test machine with a dual landing gear equipped with two 56-inch-diameter type I tires. These tests included static and drop tests with the wheels not rotating and a few drop tests with wheel pre-rotation up to 470 revolutions per minute. The tire vertical force-deflection characteristics obtained from these tests are presented and analyzed in the present paper. The effects of the following factors on the tire force-deflection characteristics are also discussed: nature of the tire air-compression process, tire hysteresis, tire centrifugal forces, and drag loads.

Although these data do not directly provide an answer to the question as to the nature of tire force-deflection characteristics under completely realistic landing conditions with a finite horizontal velocity, these data and the associated discussion do furnish background information which should be useful in studies of tire characteristics for such realistic landing conditions.

SYMBOLS

A_g	gross footprint area, sq in.
A_n	net (bearing) footprint area, sq in.
b	overall tire-ground contact width, in.
$F_{H,g}$	average instantaneous horizontal ground drag force per tire, lb
$F_{V,g}$	average instantaneous vertical ground force per tire, lb
2h	overall tire-ground contact length, in.
n	polytropic exponent
p	tire inflation pressure (gage), lb/sq in.
$\bar{p}$	tire inflation pressure (absolute), lb/sq in.

p_c	tire effective extra pressure due to carcass stiffness, lb/sq in.
r	tire radius, in.
s	shock-strut displacement
t	time
v_o	vertical velocity at ground contact, ft/sec
w	maximum free tire width, in.
W_1	weight of carriage and upper part of landing gear
W_2	weight of lower part of landing gear
W_3	weight of ground platform
x_2'	displacement of lower part of landing gear perpendicular to shock-strut axis
x_3	horizontal displacement of ground platform
z_1	vertical displacement of carriage
z_2	vertical displacement of lower part of landing gear
z_2'	displacement of lower part of landing gear parallel to shock-strut axis
z_3	vertical displacement of ground platform
δ	apparent vertical tire deflection (vertical displacement of wheel axle subsequent to ground contact), in.
δ_e	effective vertical tire deflection (difference between free tire radius and axle-to-ground distance), in.
φ	angle between shock-strut axis and vertical, deg
ω	wheel angular velocity, rpm

Subscripts:

i	instantaneous value
max	maximum

drop — drop test conditions

static — static test conditions

o — at instant of ground contact; initial condition

The use of dots over symbols indicates differentiation with respect to time.

APPARATUS, INSTRUMENTATION, AND DATA REDUCTION

The investigation was conducted in the Langley drop-test machine. Figure 1 shows a schematic drawing of this machine and the test landing gear with one of the dual wheels removed; it also shows the basic installation and the location of most of the instrumentation used for the present investigation. This machine consists of a large rigid framework in which a landing gear and supporting carriage can be lifted vertically by a hydraulic ram and then dropped upon a smooth concrete platform. Desired wheel prerotation speeds were obtained with a rotating drum driven by a variable-speed electrical motor and by supplementary air jets trained on the landing-gear wheels.

The test machine is equipped with 2 three-component strain-gage-type force-measuring dynamometers, one for measuring the forces applied to the ground platform (ⓐ in fig. 1) and one for measuring the forces applied to the carriage (ⓑ in fig. 1). In order to correct for the effects of inertia forces on these dynamometers, two accelerometers were installed on each of the three moving parts of the test setup. Accelerometers ⓒ and ⓓ (fig. 1) measure vertical and horizontal accelerations of the ground platform, respectively; accelerometers ⓔ and ⓕ, the vertical and horizontal carriage accelerations, respectively; and accelerometers ⓖ and ⓗ, the accelerations of the lower part of the landing gear in directions parallel and perpendicular to the shock-strut axis, respectively. These accelerometers had a nominal range from -10g to 10g, approximately 0.65 critical damping, and natural frequencies between 345 and 380 cycles per second.

The average instantaneous ground vertical force per tire $F_{V,g}$ can be obtained from the dynamometer and accelerometer readings by use of either of the following equations:

$$F_{V,g} = \frac{1}{2} F_{V,a} + \frac{W_3}{2g} \ddot{z}_3 \qquad (1)$$

or

$$F_{V,g} = \frac{1}{2} F_{V,b} - \frac{\eta W_1}{2g} \ddot{z}_1 - \frac{W_2}{2g} \ddot{z}_2' \cos \varphi + \frac{W_2}{2g} \ddot{x}_2' \sin \varphi \qquad (2)$$

where

$F_{V,a}$ vertical force obtained from ground dynamometer

W_3 weight of ground platform (approximately 29,000 lb)

g gravitational constant (32.2 ft/sec^2)

$\ddot{z}_3$ vertical acceleration of ground platform

$F_{V,b}$ vertical force obtained from carriage dynamometer

W_1 weight of carriage and upper part of landing gear (approximately 24,900 lb)

$\ddot{z}_1$ vertical acceleration of carriage

η fraction of carriage and upper part of landing gear below carriage dynamometer (approximately 0.20)

W_2 weight of lower part of landing gear (approximately 2,100 lb)

φ angle between shock strut axis and vertical, deg

$\ddot{z}_2'$ acceleration of lower part of landing gear parallel to shock-strut axis

$\ddot{x}_2'$ acceleration of lower part of landing gear perpendicular to shock-strut axis

A comparison of time histories of vertical ground force obtained by these two methods (eqs. (1) and (2)) is shown in figure 2 for a typical drop-test run. Good agreement between the two methods is seen to exist.

Except the data of figure 2, all vertical ground-force data presented in this paper were obtained from equation (1) inasmuch as use of this equation is believed to give more accurate results. Also it might be noted that the term $\frac{W_3}{2g} \ddot{z}_3$ in equation (1) is very small (usually less than 1,000 pounds) and is often negligible throughout most of the time

history of each drop. Consequently, the accuracy of the ground force determined by equation (1) is, to a large extent, dependent only on the accuracy of the ground platform dynamometer.

In a similar manner, the average instantaneous drag force per tire acting on the tires from the ground $F_{H,g}$ was obtained from the drag component of the ground dynamometer $F_{H,a}$ and the platform horizontal acceleration $\ddot{x}_3$ through use of the equation

$$F_{H,g} = \frac{1}{2} F_{H,a} - \frac{W_3}{2g} \ddot{x}_3 \tag{3}$$

The average tire deflection for the pair of tires δ was measured with the rack-and-gear device shown as ⓘ in figure 1. One part of this device consists of a long rack which is pinned to an L-bar attached to the ground platform in such a way that the rack is free to rotate in the plane of symmetry of the landing gear about the pin. This rack engages a gear attached near the axle of the test wheel. The gear, in turn, drives a circular slide-wire potentiometer device the output of which is linearly dependent on gear rotation. If the landing-gear shock strut is mounted vertically, the rack remains vertical during the test; thus, the device gives a direct indication of tire deflection. If the shock strut is inclined, because of the telescoping and bending of the shock strut, some tilting of the rack results and a small cosine-type error is produced. For the present tests, this tilting was less than 5° and the resultant error was insignificant.

As a check on the accuracy of the tire-deflection device, tire deflection could also be obtained from the relation

$$\delta = \Delta z_1 + \Delta s \cos \varphi \tag{4}$$

where Δz_1 is the change in carriage vertical displacement after ground contact and Δs is the corresponding shock-strut stroke (strut expansion being considered as a positive stroke). Carriage displacement was measured by a chain-and-sprocket-driven circular slide-wire potentiometer device (ⓙ in fig. 1) and strut stroke was measured by a linear slide-wire potentiometer device (ⓚ in fig. 1). Tire deflections for a typical drop obtained by direct measurement with the rack-and-gear device and by equation (4) are compared in figure 3. Fairly good agreement is seen to exist; the small disagreement which does exist is probably due to structural deflections of the landing gear and supporting carriage which are not taken into account in equation (4). Except for the data of

figure 3, all tire-deflection data presented herein were obtained from the rack-and-gear device.

Carriage vertical velocity and strut telescoping velocity were obtained from voltage-generator devices which were attached to the corresponding displacement-measuring devices.

Wheel angular velocities were obtained from voltage-generator devices attached to each of the test wheels. Wheel angular displacements were obtained from commutator-type revolution-counter devices mounted on the wheels and activated at each 12° increment of wheel rotation.

Time histories of tire pressure for the slow-speed (static) tests were obtained from two diaphragm pressure gages having a range of 0 to 250 pounds per square inch. As a check on the symmetry of the loads on the two tires, strain gages were installed on the wheel axle near each of the two wheels. All measured variables were recorded on a 36-channel oscillograph equipped with 0.01-second timing lines and utilizing galvanometers with various natural frequencies and 0.65 critical damping. All data from the dynamometers, accelerometers, and velocity-measuring devices were recorded by galvanometers which had natural frequencies of 900 cycles per second; data from tire and carriage-displacement devices, by galvanometers which had natural frequencies of 500 cycles per second; and data from the strut displacement device, by a galvanometer which had a natural frequency of 300 cycles per second. A typical test record obtained from a drop with wheel prerotation is shown in figure 4.

TEST SPECIMENS

The landing gear used in this investigation was a dual uncoupled-wheel main-landing-gear shock strut and wheel assembly from an obsolete four-engine bomber which had a gross weight of approximately 130,000 pounds. The test tires were two unused 56-inch-diameter type I (smooth contour) 16-ply nylon-cord tires with a nonskid tread pattern. A photograph of one of these tires showing the tread is given as figure 5. The radii and maximum free widths of these tires for the test inflation pressures of the present investigation are given in table I. In order to distinguish between these two tires, one tire is referred to as tire A and the other, as tire B.

TEST PROCEDURE AND EXPERIMENTAL DATA

Static Tests

A series of 19 runs was made to establish the vertical force-deflection characteristics of the test tires for conditions similar to those under which most of the generally available static tire characteristics have been obtained. These tests were made with a vertical landing-gear shock strut ($\varphi = 0^\circ$) for various vertical loadings and for initial inflation pressures p_o of 60, 80, and 100 pounds per square inch. The maximum average vertical tire deflection δ_{max} and maximum vertical ground force per wheel $F_{V,g,max}$ for each run are listed in table II. These runs required a time of several minutes per run and for this reason these tests were not, strictly speaking, static tests. However, since the time per run for these tests was much greater than that for the subsequently discussed drop tests (minutes as compared with tenths of a second), the former tests are loosely referred to herein as static tests. The ground surface for these static tests only consisted of a wooden platform installed on top of the regular concrete ground platform.

Before each run, with the shock strut partially collapsed, the tires were jacked just free of the ground platform and rotated to remove any set or flat spot on the tires which might have been left from the previous run. Then the jack was removed and, with the carriage locked in place, vertical force was applied to the tires by inflating the landing-gear shock strut by means of a hydraulic pump until the desired maximum tire loading was obtained. The strut was then slowly deflated. The total time required for the major part of each run was held to approximately 4 minutes for all but a few special runs. Sample time histories of the vertical force obtained are shown in figure 6. It might be noted that the shape of the loading curve could not be accurately controlled with the equipment available. Usually, for small vertical forces this equipment tended to give a flat-top force-time curve (for example, see run 15S in fig. 6) and for large vertical loading a pointed-top curve (for example, see run 19S in fig. 6).

The experimental results obtained from these static tests are presented in the form of plots of vertical ground force $F_{V,g}$ against tire deflection δ (figs. 7 and 8) and of tire pressure p against tire deflection δ (fig. 9).

Several special runs (runs 5S, 6S, and 7S in table II) were made to explore the effect of changing the shape of the time history of the ground force on the force-deflection curves. The time histories of vertical ground force and the tire force-deflection curves obtained from these special runs are presented in figures 10 and 11, respectively, together with data for a corresponding normal run (run 4S).

In addition, some measurements were made of the variation of ground-contact-area properties with tire deflection for one of the test tires. These data, which are presented in table III, cover the following properties of the ground-contact area: footprint length 2h, footprint width b, gross area A_g (area including the spaces between the tire treads), and net or actual bearing area A_n (area exclusive of spaces between treads).

Drop Tests Without Prerotation

A series of 18 drop tests was made without wheel prerotation and with a vertical strut ($\varphi = 0^\circ$) under almost free-fall conditions (initial acceleration of approximately 0.9g). The dropping heights varied from 0 to 3 feet and corresponded to ground-contact velocities from 0 to 12 feet per second. The initial inflation pressures were 60, 80, and 100 pounds per square inch. (It should be noted that even for an initial velocity of 0 feet per second the loading rate for the drop tests was much more rapid than for the static tests.) The tire vertical velocity at ground contact v_o, maximum tire deflection δ_{max}, and maximum vertical ground force $F_{V,g,max}$ for each run are listed in table II. Sample time histories of vertical ground force are shown in figures 2, 12, and 13 and the resulting tire vertical force-deflection curves are shown in figures 8, 13, and 14.

Drop Tests With Prerotation

Eight drop tests with various amounts of wheel prerotation were made with the landing-gear strut at an inclined position of 15° ($\varphi = 15^\circ$) at an initial inflation pressure of 80 pounds per square inch and a contact vertical velocity of approximately 8.8 feet per second. The wheel angular velocity at ground contact ω_o, maximum tire deflection δ_{max}, maximum vertical ground force $F_{V,g,max}$, and maximum drag force $F_{H,g,max}$ for these runs are listed in table IV. The sample test record shown in figure 4 was obtained from one of these runs. Sample time histories of tire deflection and vertical and drag ground forces are shown in figure 15 for two similar drops, one with prerotation and one without prerotation. The tire vertical force-deflection curves obtained are presented in figure 16.

It might be noted that the coefficients of friction between tires and ground for these prerotation tests were smaller than might normally be expected inasmuch as the concrete ground platform was contaminated by oil leakage from the shock-strut installation. This point is of some importance, since it means that the effects of drag load on the vertical

force-deflection characteristics for the present data obtained on oil-contaminated concrete may be slightly different from these effects for data that would be obtained on completely dry concrete.

The prerotation drop tests also furnished some data on the growth of the tire radius due to centrifugal forces since the difference in the readings of the tire-deflection device (fig. 1) at the instant of ground contact for runs with and without prerotation is a direct measure of the change in the radius. The data obtained by this procedure for the runs in table IV and some additional unpublished data for these same tires are plotted in figure 17.

Wheel Symmetry For All Testing

In all the preceding tests, the orientations of the two test wheels were made as symmetric as possible. However, as a result of a slight misalinement of the wheel axle with the ground platform surface and slight differences in the radii of the two test tires, the two tires did not hit the ground at exactly the same time during testing and, consequently, there was usually a small difference between the vertical loads for the two tires. In order to obtain some idea of the size of this difference, the readings of the strain gages installed on the wheel axle near each of the two wheels were examined. From the data obtained from these gages and from visual observations, it appeared that the overall difference in vertical load for the two tires was usually equivalent to a difference of somewhat less than 0.1 inch for the two tire deflections. For some runs tire A had more load than tire B whereas for other runs this situation was reversed.

DISCUSSION

Static Tests

Tire vertical force-deflection characteristics.- Most of the static force-deflection curves shown in this paper are used as a standard for comparison with the dynamic test curves and, for the most part, they contain no special points of interest in themselves. The only static curves which might be of some slight interest in themselves are those in figure 11. (See also fig. 10.) Figure 11 shows that the size and shape of the hysteresis loop depends to some extent on the shape of the loading time-history curve and also indicates the nature of the force-deflection variation following a reversal of the direction of loading subsequent to the occurrence of a minimum force position in the force time history.

Pressure change.- The variation of tire inflation pressure p with vertical tire deflection δ from the static tests (fig. 9) appears to agree substantially with the following relation originally proposed by Michael in reference 1:

$$p = p_o + \kappa \bar{p}_o \left(\frac{\delta}{w}\right)^2 \tag{5}$$

where p_o is the initial gage pressure, $\bar{p}_o$ is the initial absolute pressure, w is the tire maximum free width, and κ is a constant which the experimental data of figure 9 indicates to be approximately equal to 0.66 for tire A and 0.61 for tire B. (See solid and dashed lines in fig. 9.) It might be of interest to note that, by analyzing the experimental data of reference 2 for two other type I tires having diameters of 27 inches and 44 inches, a value of κ of 0.66 was found for both tires. It might also be noted that, although there appears to be a slight hysteresis effect in the experimental data of figure 9, it is hard to say whether this is entirely an actual tire effect or whether it is in part due to hysteresis effects in the tire pressure gages. In any event, this particular hysteresis effect is probably of no great practical importance.

Tire Vertical Force-Deflection Characteristics

For Drop Tests Without Prerotation

The tire vertical force-deflection curves shown in figure 14 for the case of vertical drops without wheel prerotation are seen to give, for each initial inflation pressure, the same variation of force with deflection for increasing force, regardless of the initial vertical velocity, for a range of initial velocity from 0 to 11.9 feet per second. In view of this observation, which is also supported by the data of reference 3 for a 27-inch-diameter type I tire for initial velocities between 5.8 and 11.6 feet per second, it appears reasonable to conclude that, in general, for drop tests without prerotation and for increasing force, the variation of vertical force with tire deflection is substantially independent of initial vertical velocity.

Some idea of the nature of the vertical force-deflection variation following a reversal of the direction of loading (other than that at the first peak load) is shown in figure 13 for two drops where such a reversal occurs. It may be noted that, after this force reversal and for subsequent increasing force, the curves do not immediately return to the increasing-force curves for the initial parts of the time histories.

Drop Tests With Prerotation

Tire vertical force-deflection characteristics.- The variations of tire vertical ground force with tire deflection obtained from the vertical drops with wheel prerotation (fig. 16) contain the following interesting features:

For zero prerotation, the tire stiffness (defined here as $F_{V,g}/\delta$) is seen to be a maximum and for the most part the stiffness tends to decrease with increasing prerotation speed. For that part of the prerotation drops where the wheels are still spinning (see parts of test curves to the left of the respective symbols), all the curves appear to be approximately the same curve and this mean curve is seen to lie somewhere inside the hysteresis loop for the vertical drops without prerotation. Since the test data cover a considerable range of angular velocity (up to 470 revolutions per minute), it appears reasonable to conclude that, for a given inflation pressure, the variation of vertical ground force with tire deflection for a rotating tire has a definite form which is largely independent of the magnitude of the particular angular velocity involved and that the stiffness of the tire for this rotating condition is less than that for the case of a vertical drop without wheel prerotation.

Subsequent to the stopping of the wheels (see parts of curves to the right of the respective test symbols in fig. 16), the force-deflection curves are seen to break away from the mean curve for a rotating tire and then, as would be expected, rise up to approach the solid-line curve for a vertical drop without prerotation.

Tire-radius change.- From the experimental data in figure 17, it appears that the tire-radius change due to wheel angular velocity is roughly proportional to the square of the wheel angular velocity (see solid-line curve in fig. 17), the radius change being approximately 0.2 inch at 500 revolutions per minute (corresponding to approximately 84 miles per hour). This type of velocity-squared variation was previously demonstrated by Davidson and Hadekel (ref. 4) and has also been confirmed by some unpublished NACA data for several other tires.

COMPARISON OF DIFFERENT EXPERIMENTAL FORCE-DEFLECTION VARIATIONS

The force-deflection curves for static tests, for drop tests without prerotation, and for the early stages of the prerotation drop tests (before wheel stopping) are compared with each other in figures 8 and 18. It may be seen from these figures that, on the average, for increasing

force the tire stiffness $F_{V,g}/\delta$ for drop tests without wheel prerotation is appreciably greater than that for the static tests and that the stiffness for the rotating-tire case is almost the same as that for the static case. The following simplified theoretical considerations are presented to attempt to clarify some of the basic differences between tire vertical force-deflection characteristics for different types of landing conditions.

Effects of Centrifugal Forces

For the first consideration, it is assumed that the only important factors influencing tire vertical force-deflection characteristics are the tire elastic stiffness and the centrifugal growth of the tire radius due to wheel rotation; tire hysteresis effects, drag load effects, and other inertia effects are neglected.

It is important to distinguish between two types of tire deflection which will be referred to as apparent tire deflection δ and effective tire deflection δ_e. The apparent tire deflection δ is defined as the change in wheel-axle height subsequent to ground contact $(\delta = z_2 - z_{2,o})$ and the effective tire deflection δ_e is defined as the difference between the instantaneous free tire radius and the wheel axle-to-ground distance. Because of the change in wheel angular velocity during a landing involving wheel rotation, these two definitions are not identical or, more specifically, the two types of tire deflection are related by the equation

$$\delta_e = \delta + r - r_i \tag{6}$$

where r is the instantaneous free tire radius (which depends on the angular velocity ω) and r_i is the instantaneous free radius at the instant of ground contact. It should be noted that the effective tire deflection is a direct measure of tire distortion whereas the actual tire deflection is not. On the other hand, in order to make time-history solutions of the equations of motion for a landing gear, it is necessary to deal with the absolute positions of the wheels in space, which are represented by the apparent tire deflection and not by the effective tire deflection.

Within the scope of the preceding considerations, the tire vertical ground force $F_{V,g}$ will depend only on the centrifugal forces (proportional to the square of the angular velocity ω^2) and on the effective tire deflection in the manner

$$F_{V,g} = f(\omega^2,\delta_e) = f(\omega^2,\delta+r-r_i)$$

where $f(\omega^2,\delta_e)$ is an increasing function of δ_e.

By expansion of this equation into a Taylor series with respect to the static condition $f(0,\delta)$ and by dropping all terms except first-order terms, this equation takes the form

$$F_{V,g} = \left(F_{V,g}\right)_{\substack{\delta=\delta_e \\ \omega=0}} + \left(\frac{\partial F_{V,g}}{\partial \omega^2}\right)_{\delta=\delta_e} \omega^2 + \left(\frac{\partial F_{V,g}}{\partial \delta_e}\right)_{\omega=0} \Delta r \qquad (7)$$

where Δr is the change in tire radius subsequent to ground contact ($\Delta r = r - r_i$). The first term on the right-hand side of equation (7) represents the tire static stiffness; the second term, the change in stiffness due to centrifugal forces; and the third term, an apparent change in tire stiffness which is seen to arise from the distinction between effective and apparent tire deflections. The importance and variation of the second term is unknown. The significance of the other two terms can be examined with the aid of the following sketch for three different types of landing conditions. The abscissa of this plot is the apparent tire deflection and the ordinate is the sum of the first and third terms on the right-hand side of equation (7).

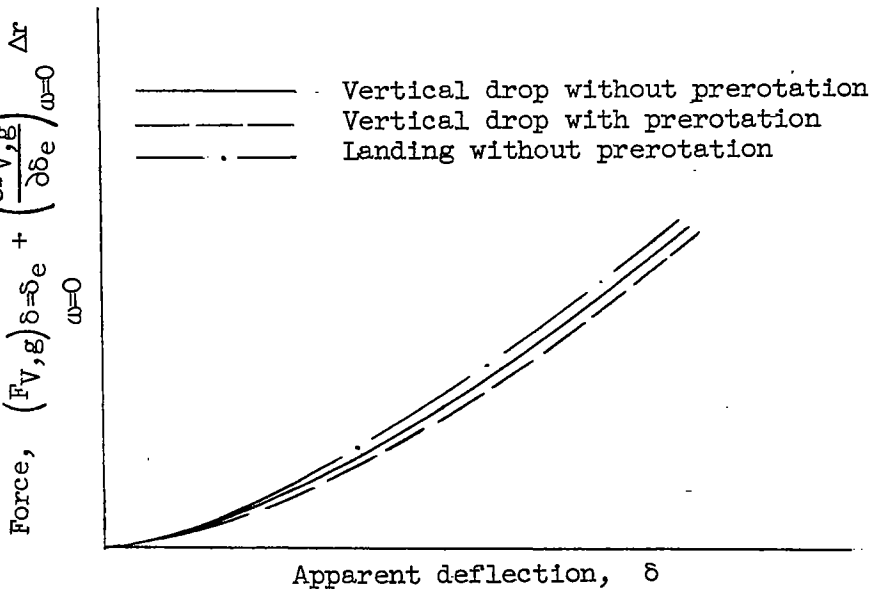

For a vertical drop without prerotation, the solid line applies. For a vertical drop with prerotation (dashed line), until the wheel angular

velocity begins to decrease appreciably, the vertical force-deflection curve will be the same as for the drop without prerotation; as the wheel angular velocity decreases to zero, however, the radius change eventually becomes equal to a constant negative amount and the force-deflection curve will consequently become parallel to and below the corresponding curve for a drop without prerotation. (See eq. (7).) In contrast, for the case of a landing with horizontal velocity and no prerotation, the tire radius grows after ground contact during wheel spin-up ($\Delta r > 0$) and the force-deflection variation will consequently be similar to that given by the dash-dot curve in the sketch.

In order to give some idea of the order of magnitude of this effect, it may be observed from figure 17 that for an angular velocity of 500 revolutions per minute (corresponding to approximately 84 miles per hour) the radius change is about 0.2 inch; hence, for these conditions, the right-hand sections of the upper and lower curves in the preceding sketch would be horizontally displaced by a distance of 0.4 inch.

Hysteresis Effects

Hysteresis effects are probably responsible for much of the difference between dynamic force-deflection characteristics for rotating and nonrotating tires. This observation can be easily supported by considering the case of a wheel the peripheral velocity of which is so much larger than the vertical velocity that the rotational motion completely predominates over the vertical motion. For this case which approaches the pure rolling condition, no hysteresis loop exists. (See, for example, the experimental evidence of ref. 5.) It then seems reasonable to conclude that the force-deflection curve for a rapidly rotating tire during a drop or a landing is some weighted mean of the increasing-force and decreasing-force branches of the force-deflection curves for a drop test without prerotation; for less rapid rotation some intermediate condition will exist. This latter conclusion is seen to be supported by the experimental data of figure 16. Moreover, as was previously noted, the parts of the curves in figure 16 which correspond to the rotating-tire conditions appear to be independent of rotational speed for the range of speeds shown (40 to 470 revolutions per minute); hence, all the rotating-tire data in figure 16 can probably be considered to correspond to the limiting condition where the rotational motion of the tires predominates over their vertical motion and where no hysteresis loop exists.

Drag Load Effects

Another factor which may influence the vertical force-deflection relation is the drag force which appears during prerotation drop tests and in actual landings. It is known from static tests that, if a drag

load is applied to a tire with a given vertical loading, it tends to sink (ref. 2) or, if this effect is interpreted in terms of tire stiffness, it can be said that a tire becomes less stiff in the vertical direction under the action of drag loads. Although no quantitative estimate can be made of the size of this effect for the present tests, it might be noted that static tests for a different type and stiffer tire of the same size gave a change of vertical deflection due to drag of about 0.1 inch. (See ref. 2.)

Pressure-Rise Effects

In order to explain the difference between force-deflection curves for static and drop tests without wheel rotation, Michael (ref. 1), Rotta (ref. 6), and Hadekel (ref. 4) have used arguments similar to the following:

First consider the pressure change in a tire due to tire deflection. It is assumed that the change of air volume in a tire depends only on tire deflection δ or

$$\frac{V_o}{V} = 1 + f_1(\delta) \tag{8}$$

where

V air volume

V_o initial air volume

$f_1(\delta)$ function of δ which approaches zero as $\delta \rightarrow 0$

Then, from the gas law for a polytropic process,

$$\frac{\bar{p}}{\bar{p}_o} = \left(\frac{V_o}{V}\right)^n \tag{9}$$

where

$\bar{p}$ absolute inflation pressure

$\bar{p}_o$ initial absolute inflation pressure

n polytropic exponent

Thus, from the substitution of equation (8) into equation (9),

$$\frac{\overline{p}}{\overline{p}_o} = \left[1 + f_1(\delta)\right]^n \tag{10}$$

Expansion of the right-hand side of equation (10) into a power series and omission of high-order terms yields

$$\frac{\overline{p}}{\overline{p}_o} = 1 + nf_1(\delta)$$

or, in terms of gage pressure, the pressure change Δp is

$$\Delta p = \overline{p} - \overline{p}_o = p - p_o = n\overline{p}_o f_1(\delta) \tag{11}$$

For a static test, where the process is essentially isothermal, $n = 1$ and equation (11) gives for the pressure change due to tire deflection

$$\Delta p_{static} = \overline{p}_o f_1(\delta) \tag{12}$$

For drop tests the pressure change is probably neither isothermal nor adiabatic but corresponds to some intermediate condition ($1.0 < n < 1.4$) according to the relation $\Delta p_{drop} = n\overline{p}_o f_1(\delta)$ (from eq. (11)). Combination of this relation with equation (12) gives

$$\Delta p_{drop} = n\,\Delta p_{static} \tag{13}$$

Next consider the ground force $F_{V,g}$. The ground force is equal to the product of gross ground contact area A_g and the sum of the inflation pressure p and a small correction factor p_c which takes into account the tire carcass stiffness in terms of an effective extra pressure. (See ref. 4 or ref. 6.)

$$F_{V,g} = (p + p_c)A_g \tag{14}$$

From equations (11), (13), and (14) and the assumption that area is a function of tire deflection alone, the vertical ground force for drop tests can be expressed in terms of the corresponding value for static tests as

$$\frac{F_{V,g,drop}}{F_{V,g,static}} = \frac{p_o + n\,\Delta p_{static} + p_c}{p_o + \Delta p_{static} + p_c} \tag{15}$$

The calculated variation of $F_{V,g,drop}$ from the experimental static data of figures 7 and 9 according to equation (15) are compared with the corresponding experimental variations in figure 18 for initial pressures of 60 and 100 pounds per square inch. (A value of p_c = 8 pounds per square inch was used in these calculations and is based on an extensive unpublished study of tire static properties.) For these conditions, the actual value of the polytropic constant n is not known. However, it is apparent from equation (15) that the maximum effect of pressure rise for drop tests will occur if the process is adiabatic. The calculated curves of figure 18 were computed on this basis (n = 1.4). Notwithstanding, it can be noted in figure 18 that the differences between the static-test data and the corresponding calculated drop-test data are small. It may also be noted from the comparisons in figure 18 that the calculated forces are usually smaller than the corresponding experimental forces; consequently, it appears that the difference between static and drop-test data is due not only to difference in the air-compression process for the two cases but also to other causes.

CONCLUSIONS

This paper has presented and compared experimental vertical force-deflection characteristics for a pair of 56-inch-diameter tires under static conditions and drop-test conditions with and without prerotation. These data indicate the following conclusions which appear to be valid at least for the range of conditions tested.

1. For drop tests without prerotation, the tire vertical force-deflection characteristics for increasing force appear to be substantially independent of initial vertical velocity.

2. For drop tests with prerotation up to 470 revolutions per minute, the tire vertical force-deflection characteristics appear to be largely independent of the magnitude of wheel angular velocity as long as the wheels remain rotating.

3. There is a small but noticeable difference between the tire vertical force-deflection characteristics for the different test conditions. Generally speaking, for increasing force, the tires are found to be least stiff for static tests, almost the same as for the static case for prerotation drops as long as the tires remain rotating, and appreciably stiffer for drop tests without prerotation.

Langley Aeronautical Laboratory,
National Advisory Committee for Aeronautics,
Langley Field, Va., October 10, 1956.

REFERENCES

1. Michael, Franz: The Problem of Tire Sizes for Airplane Wheels. NACA TM 689, 1932.

2. Horne, Walter B.: Static Force-Deflection Characteristics of Six Aircraft Tires Under Combined Loading. NACA TN 2926, 1953.

3. Milwitzky, Benjamin, and Cook, Francis E.: Analysis of Landing-Gear Behavior. NACA Rep. 1154, 1953. (Supersedes NACA TN 2755.)

4. Hadekel, R.: The Mechanical Characteristics of Pneumatic Tyres. S & T Memo. No. 5/50, British Ministry of Supply, TPA 3/TIB, Mar. 1950.

5. Schippel, H. F.: Airplane Tires and Wheels. Aero. Eng., Trans. A.S.M.E., vol. 3, no. 1, Jan.-Mar. 1931, pp. 45-52.

6. Rotta, J.: Properties of the Aeroplane During Take-Off and Alighting. Reps. and Translations No. 969, British M.A.P. Völkenrode, Dec. 15, 1947.

TABLE I.- TIRE RADIUS AND WIDTH

[At equilibrium conditions]

	Pressure, p_o, lb/sq in.	Radius, in.	Maximum width, in.
Tire A	60	28.2	19.8
	80	28.3	19.8
	100	28.4	19.9
Tire B	60	28.3	19.8
	80	28.4	19.8
	100	28.5	19.9

TABLE II.- TEST CONDITIONS FOR STATIC RUNS AND DROP TESTS WITHOUT PREROTATION

$[\varphi = 0^{\circ}]$

Run (a)	p_o, lb/sq in.	δ_{max}, in.	v_o, ft/sec	$F_{V,g,max}$, lb
1S	60	5.6	----	30,000
2S	60	6.2	----	33,000
3S	60	7.0	----	39,000
4S	60	7.6	----	44,000
[b]5S	60	7.7	----	44,000
[b]6S	60	7.6	----	44,000
[b]7S	60	7.7	----	44,000
8S	60	8.2	----	47,000
9S	60	8.7	----	51,000
10S	80	5.1	----	34,000
11S	80	6.6	----	45,000
12S	80	7.2	----	50,000
13S	80	7.5	----	53,000
14S	80	8.6	----	63,000
15S	100	4.6	----	36,000
16S	100	5.3	----	44,000
17S	100	5.9	----	50,000
18S	100	7.5	----	65,000
19S	100	8.6	----	77,000
1D	60	4.9	0.7	27,000
2D	60	6.0	3.5	34,000
3D	60	6.7	4.9	40,000
4D	60	7.3	5.8	45,000
5D	60	7.8	7.0	50,000
6D	60	8.1	7.6	52,000
7D	80	3.8	0.0	27,000
8D	80	5.5	4.2	39,000
9D	80	6.2	5.5	45,000
10D	80	6.8	6.8	50,000
11D	80	7.2	7.4	55,000
12D	80	8.2	9.9	64,000
13D	100	3.3	0.0	26,000
14D	100	4.5	4.0	38,000
15D	100	6.0	6.3	52,000
16D	100	6.2	7.0	55,000
17D	100	7.3	9.8	67,000
18D	100	8.4	11.9	78,000

[a]S indicates static tests; D indicates drop tests without prerotation.

[b]Special runs made to explore the effect of changing the shape of the time history of the ground force on the force-deflection curves.

TABLE III.- FOOTPRINT DATA FOR TIRE B

p_o, lb/sq in.	p, lb/sq in.	$F_{V,g}$, lb	δ, in.	A_g, sq in.	A_n, sq in.	b, in.	2h, in.
61	(a)	7,200	1.79	141.6	84.8	10.3	17.0
60	62	13,200	2.73	198.0	119.3	11.6	20.0
62	64	19,200	3.67	286.6	169.5	14.0	24.1
61	(a)	25,500	4.67	366.0	226.3	15.7	27.5
60	(a)	30,300	5.39	428.7	253.5	16.6	29.1
60	(a)	39,500	6.70	549.0	323.6	19.4	32.6

[a]Value not measured.

TABLE IV.- TEST CONDITIONS FOR DROP TESTS WITH PREROTATION

$[\varphi = 15^\circ;\ p_o = 80$ lb/sq in.; $v_o \approx 8.8$ ft/sec$]$

Run	ω_o, rpm	δ_{max}, in.	$F_{V,g,max}$, lb	$F_{H,g,max}$, lb
1P	0	8.1	63,000	------
2P	40	8.2	63,000	5,000
3P	180	8.2	62,000	13,000
4P	240	8.1	62,000	14,000
5P	0	8.0	63,000	------
6P	380	8.2	58,000	16,000
7P	0	8.0	62,000	------
8P	470	8.1	57,000	16,000

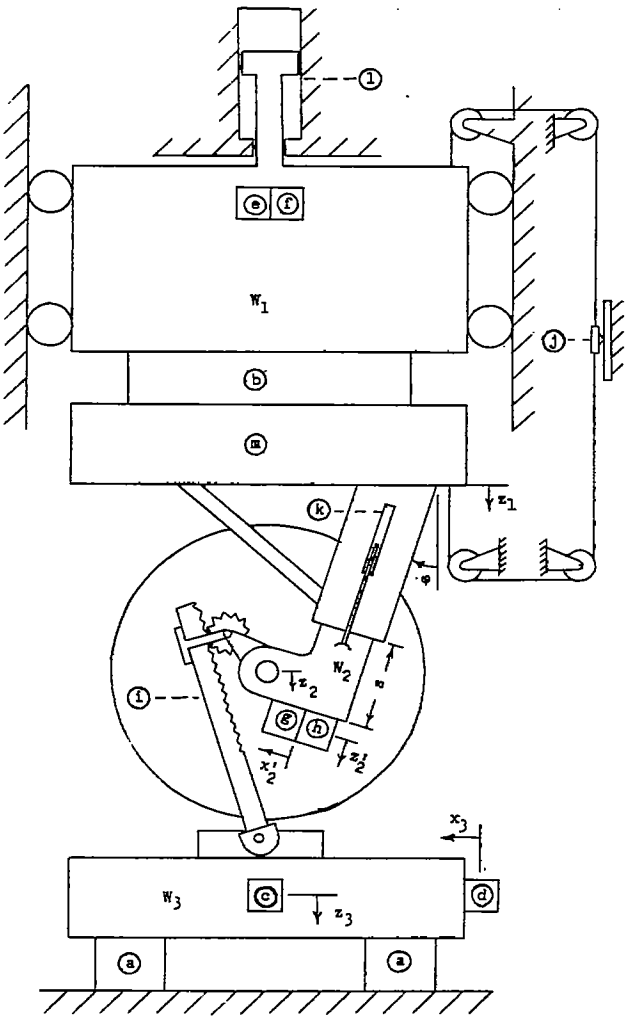

ⓐ Platform dynamometer
ⓑ Carriage dynamometer
ⓒ Platform vertical accelerometer
ⓓ Platform horizontal accelerometer
ⓔ Carriage vertical accelerometer
ⓕ Carriage horizontal accelerometer
ⓖ Wheel axial accelerometer
ⓗ Wheel normal accelerometer
ⓘ Tire-deflection measuring device
ⓙ Carriage displacement and velocity device
ⓚ Strut-displacement and velocity device
① Hydraulic ram
ⓜ Landing-gear attachment fitting

Figure 1.- Schematic drawing of Langley drop-test machine.

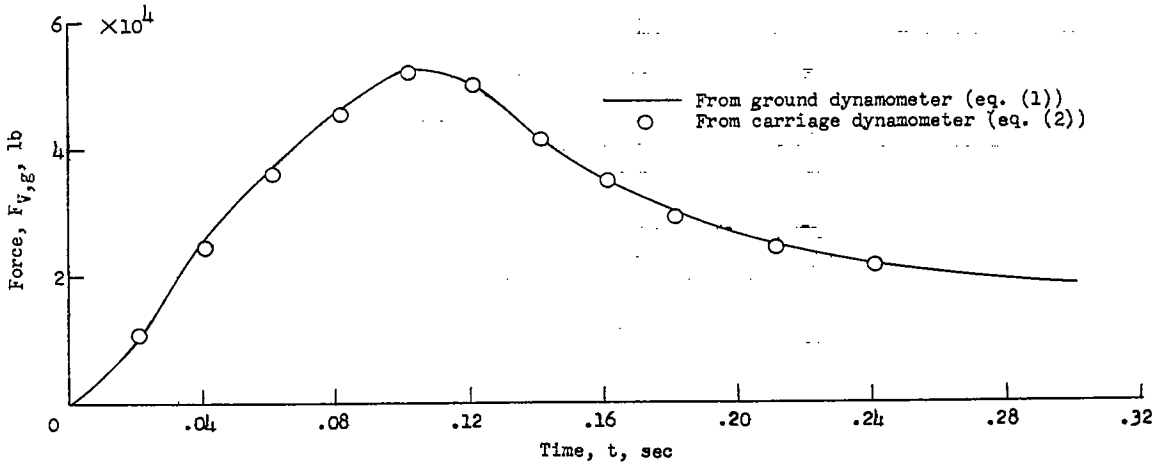

Figure 2.- Typical comparison of experimental drop-test time histories of vertical ground force obtained by two different methods. Run 15D: p_o = 100 lb/sq in.; v_o = 6.3 ft/sec.

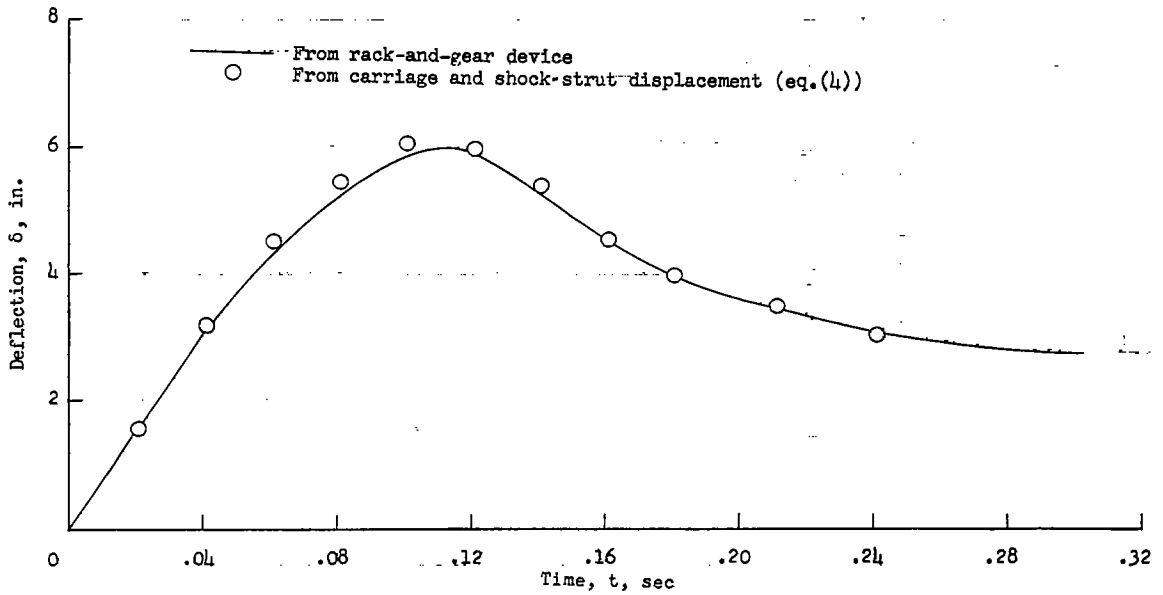

Figure 3.- Typical comparison of experimental drop-test time histories of vertical tire deflection obtained by two different methods. Run 15D: p_o = 100 lb/sq in.; v_o = 6.3 ft/sec.

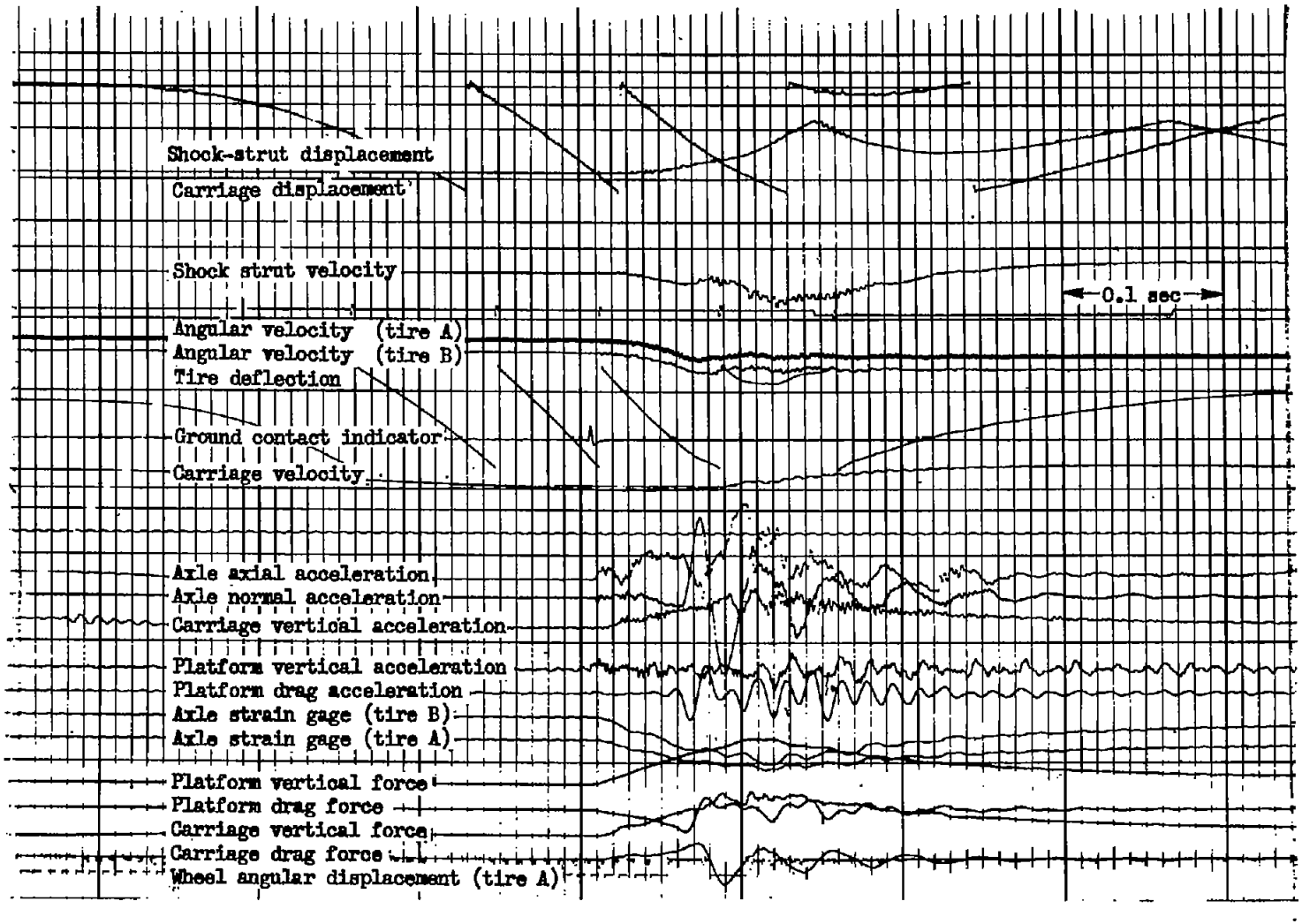

Figure 4.- Sample test record for drop test with prerotation. Run 4P: $\varphi = 15^{\circ}$; $p_o = 80$ lb/sq in.; $v_o \approx 8.8$ ft/sec; $\omega_o = 240$ rpm.

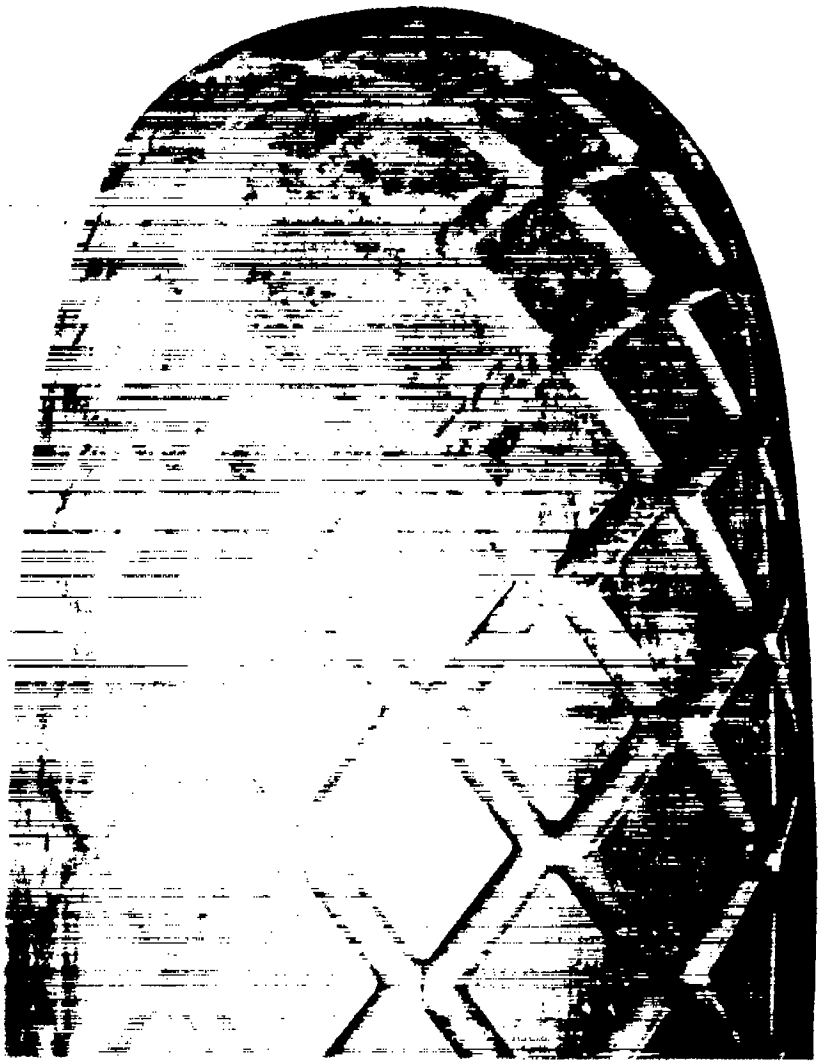

L-93907.1

Figure 5.- Photograph showing tread detail for the test tires.

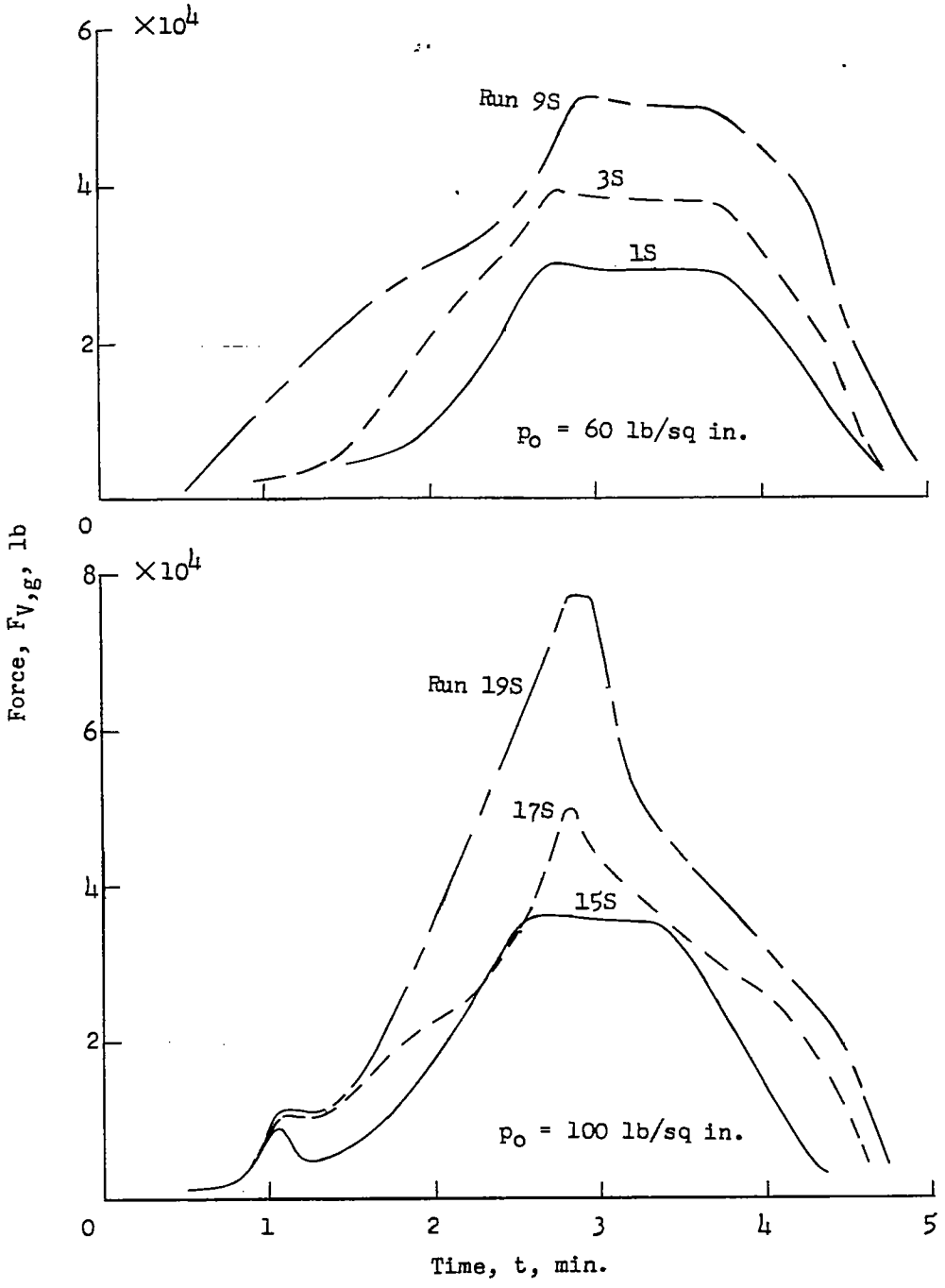

Figure 6.- Time histories of vertical ground force for typical static runs.

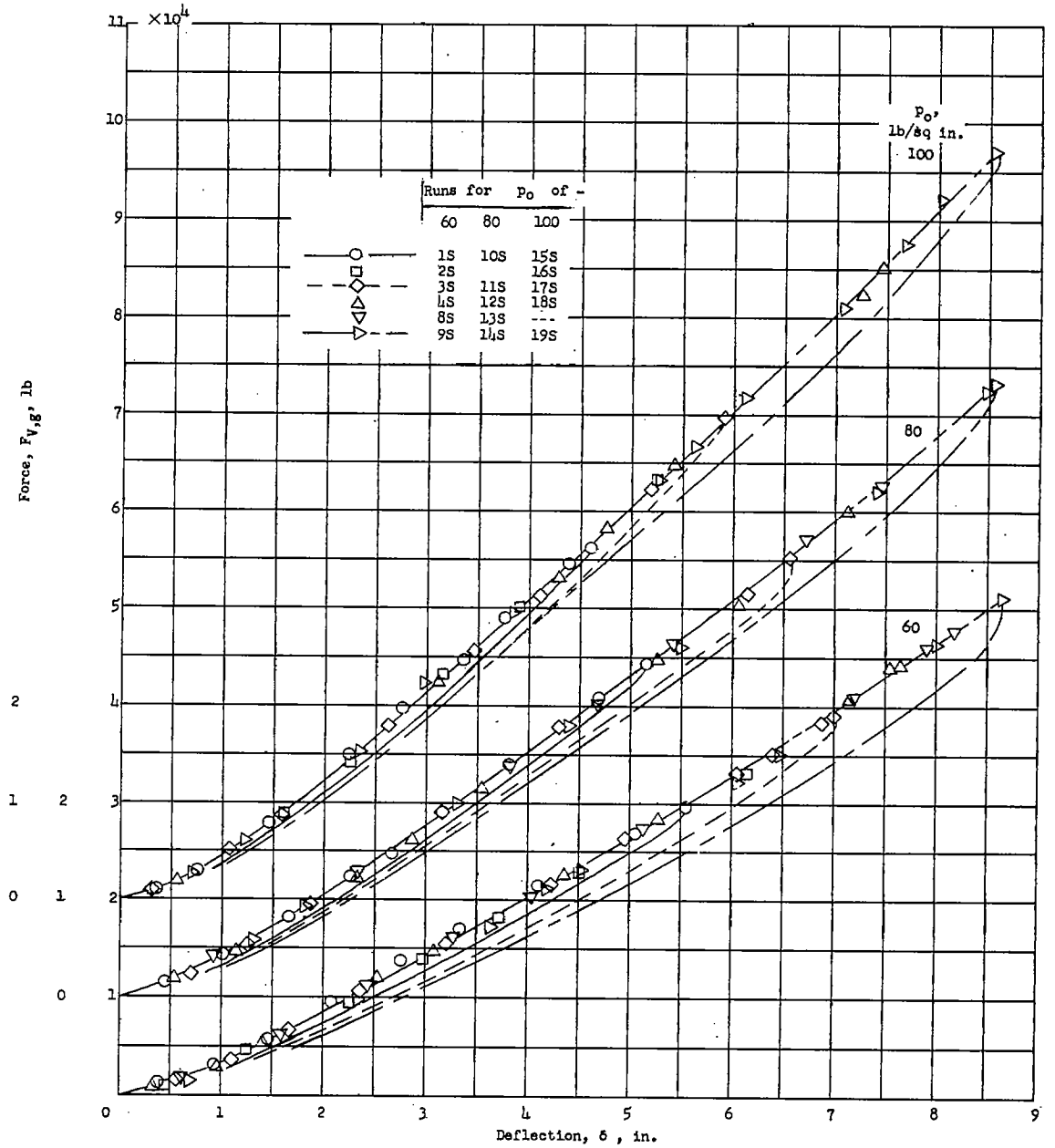

Figure 7.- Variation of vertical ground force with vertical tire deflection obtained from static tests.

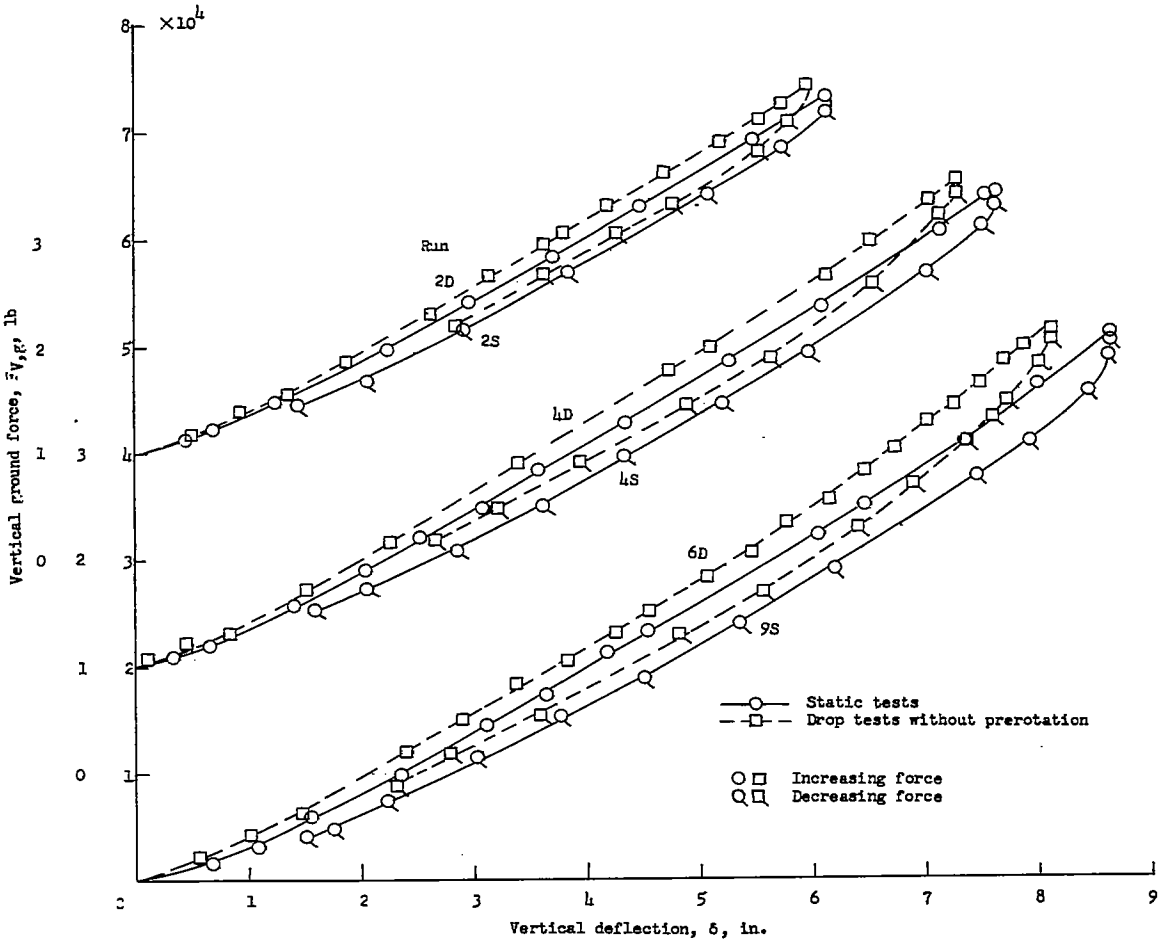

(a) p_o = 60 lb/sq in.

Figure 8.- Comparison of force-deflection curves at several tire inflation pressures for static tests and drop tests without prerotation.

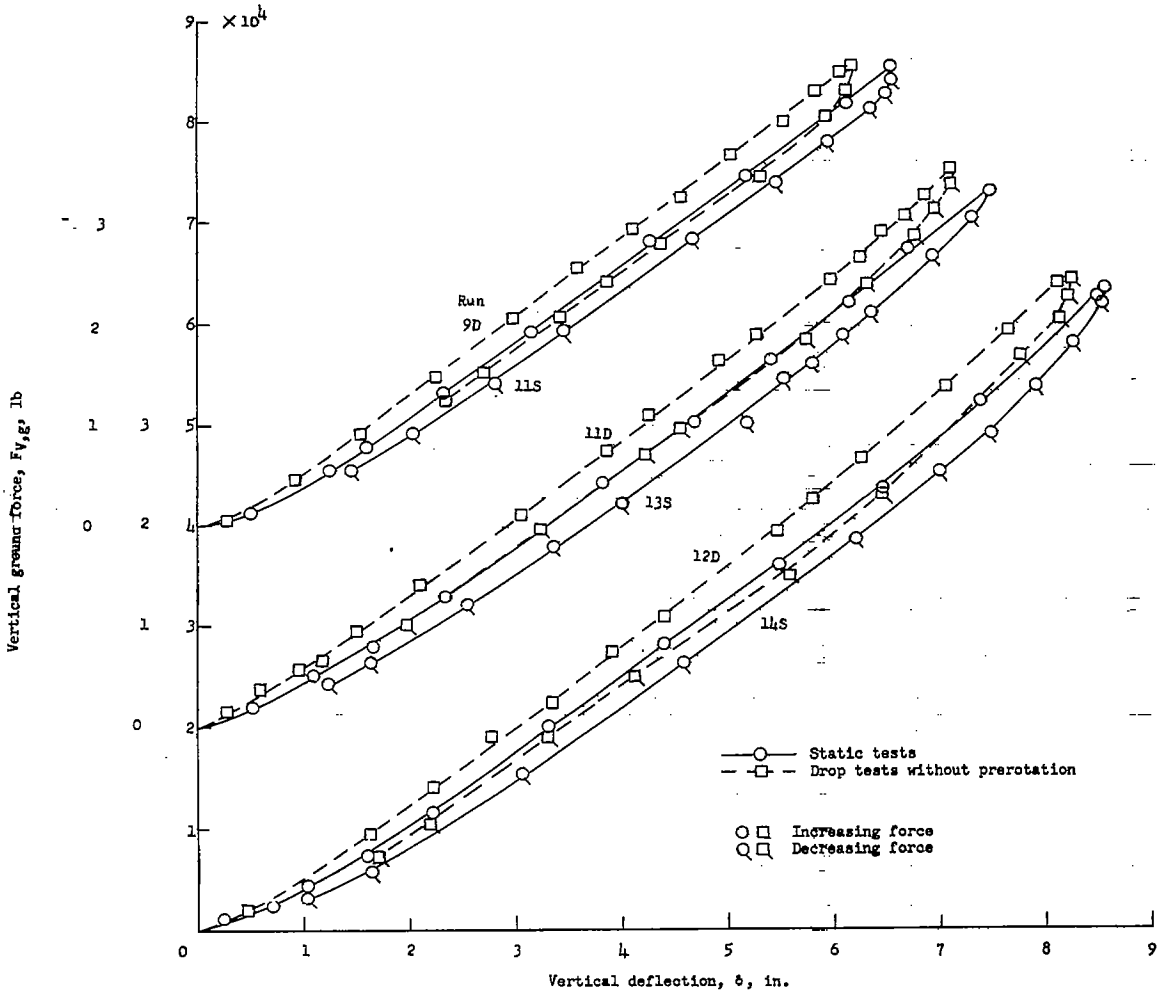

(b) p_o = 80 lb/sq in.

Figure 8.- Continued.

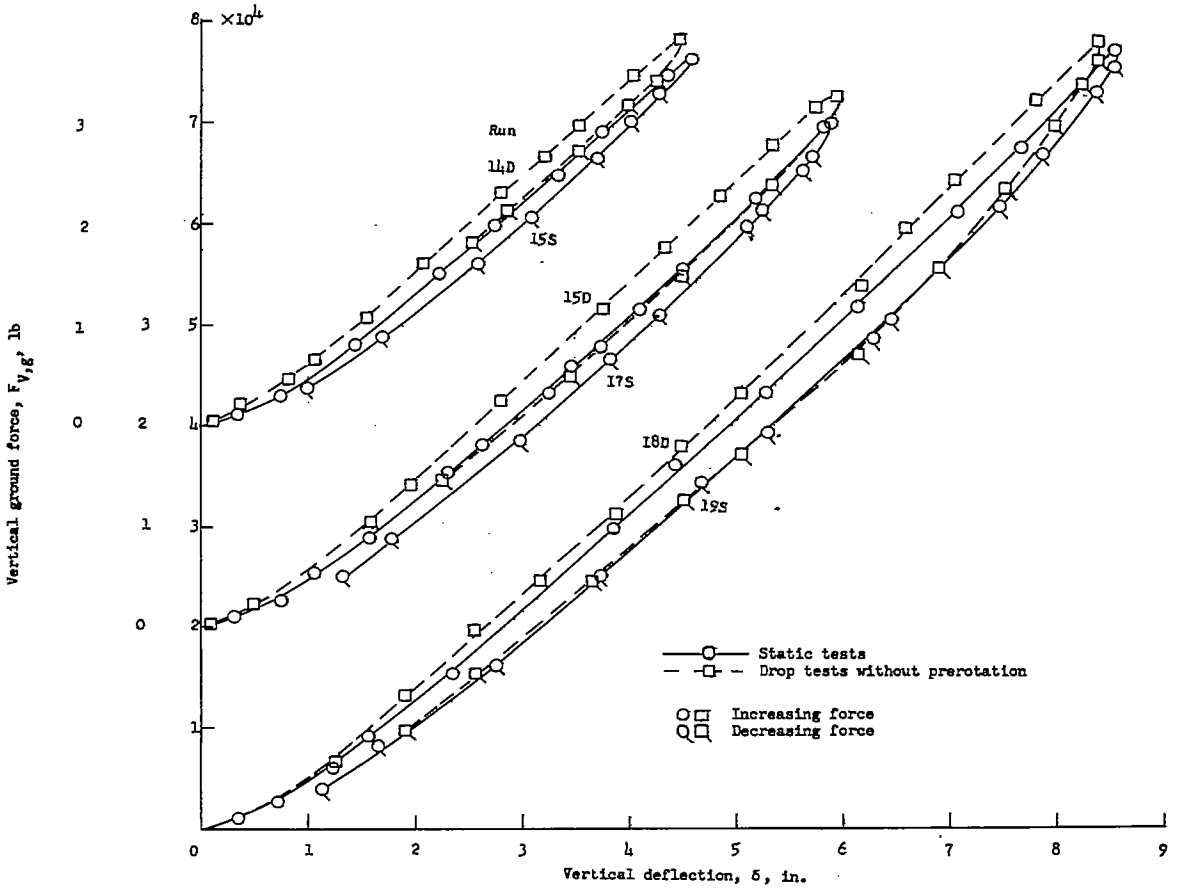

(c) p_o = 100 lb/sq in.

Figure 8.- Concluded.

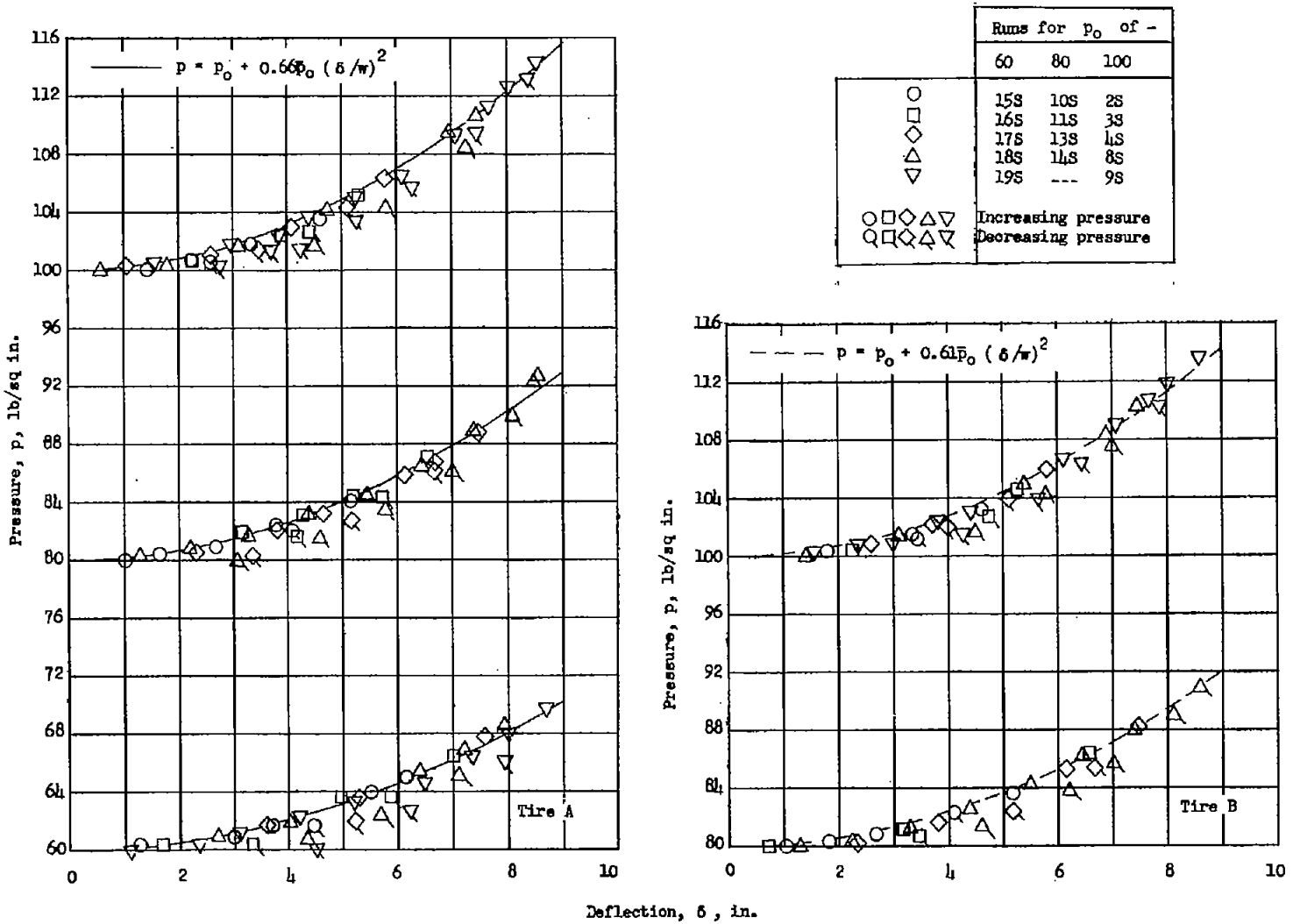

Figure 9.- Variation of tire inflation pressure with vertical tire deflection obtained from static test data.

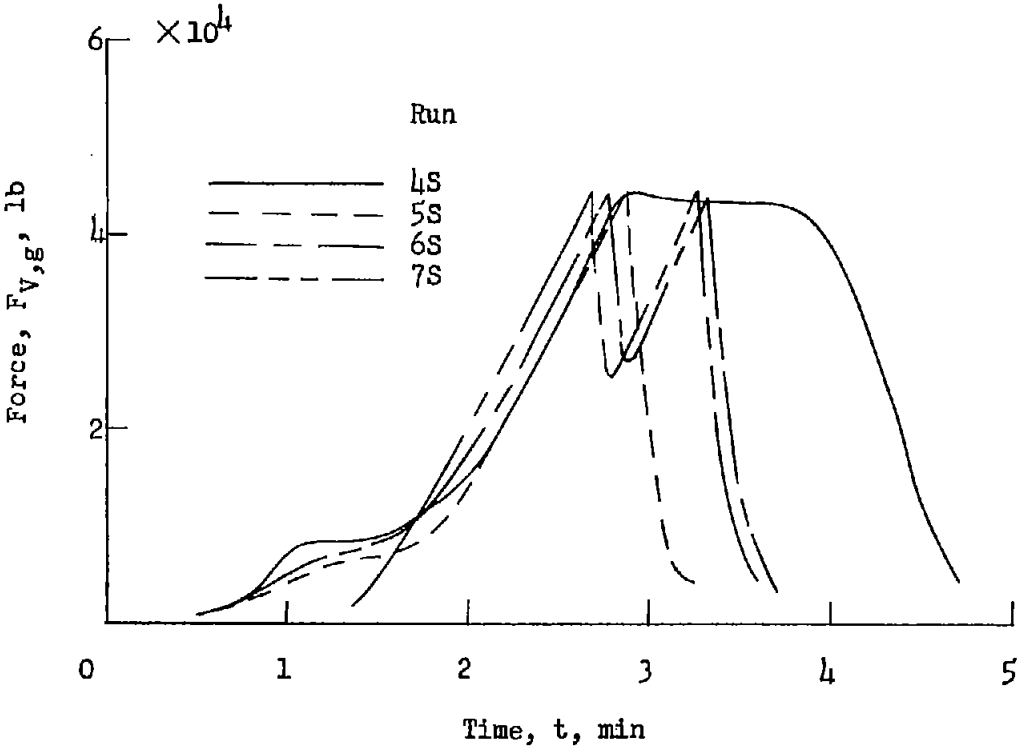

Figure 10.- Time histories of vertical ground force for several special static runs.

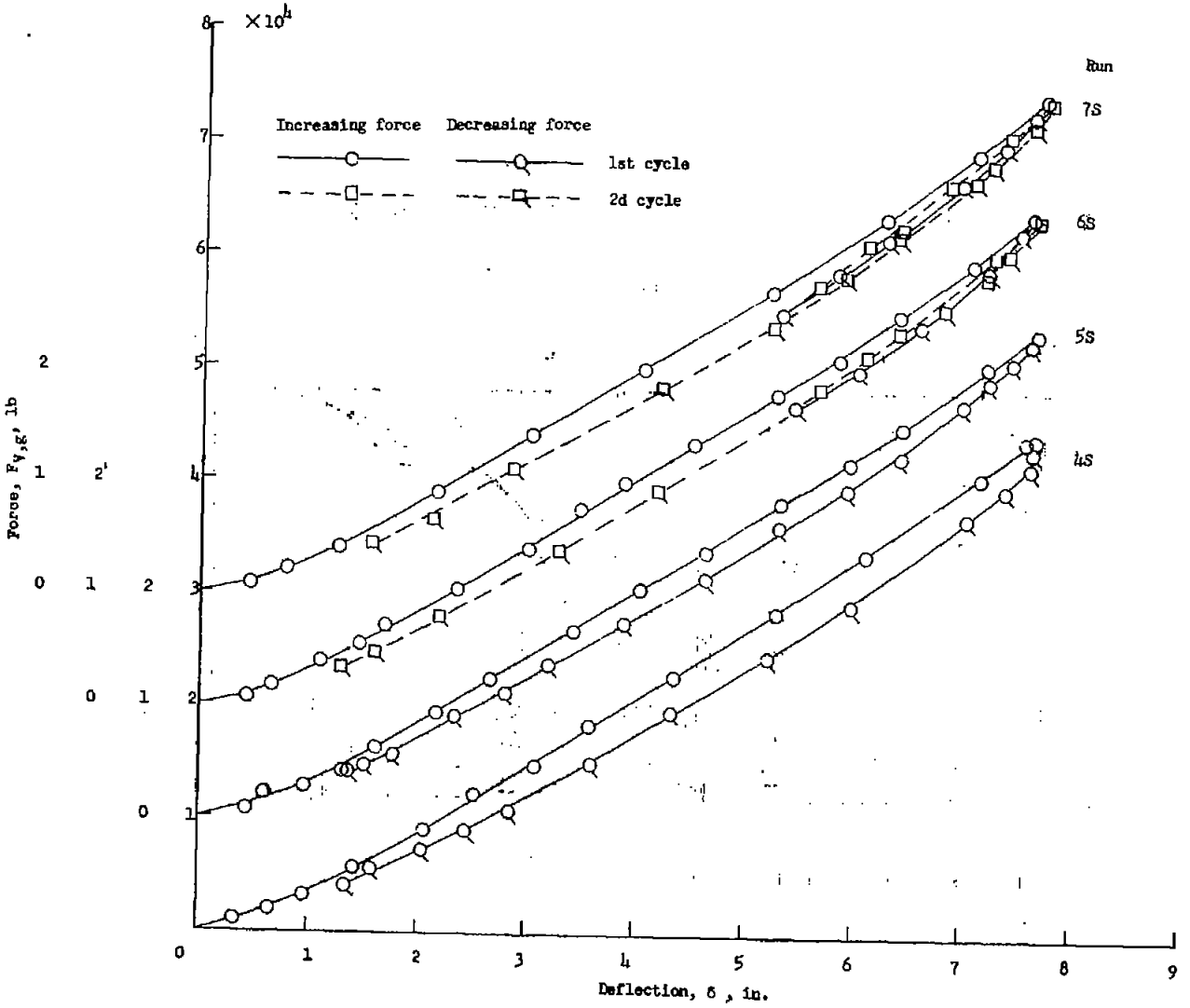

Figure 11.- Force-deflection curves for four special static runs.

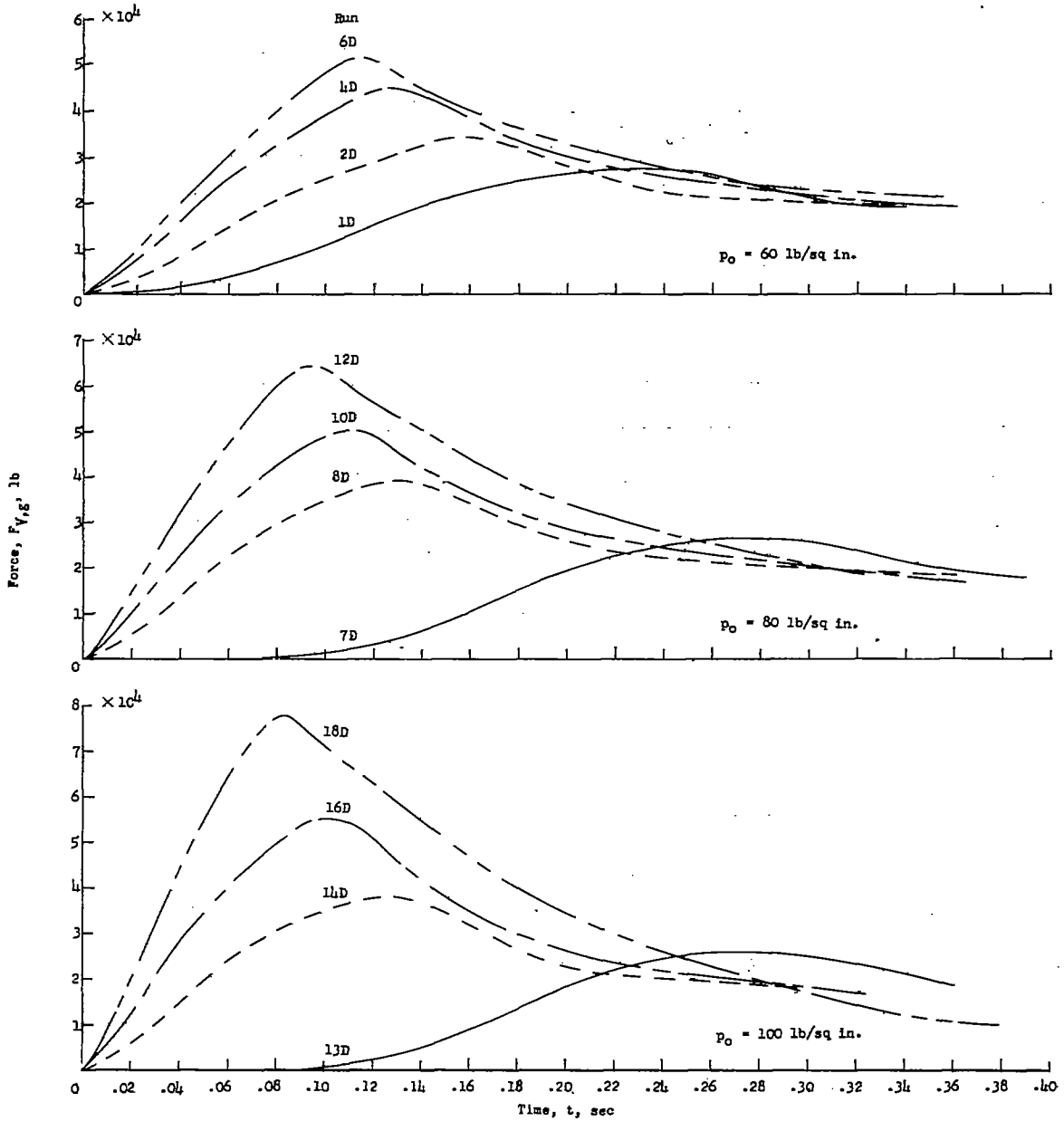

Figure 12.- Time histories of vertical ground force for typical drops without wheel prerotation.

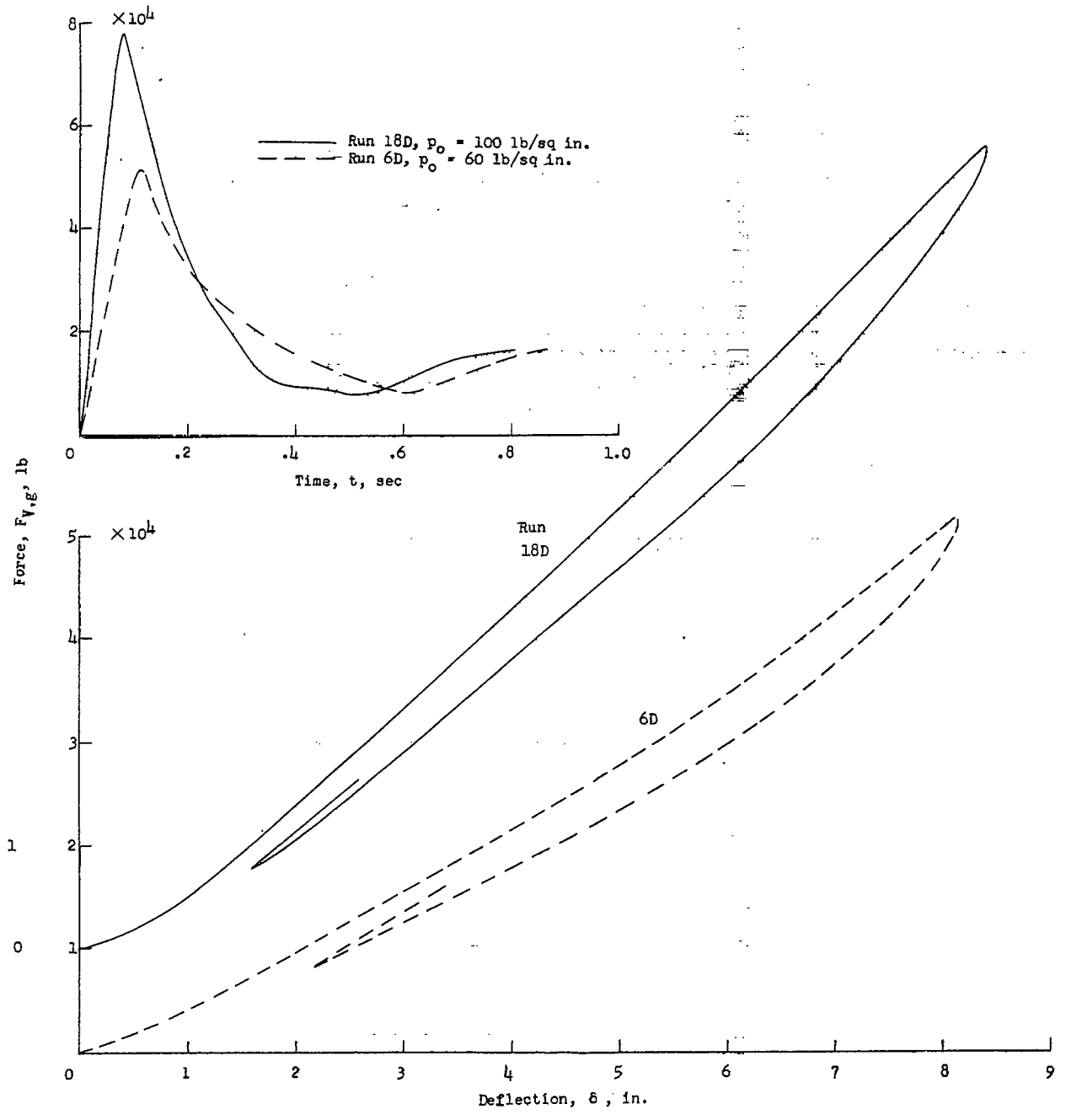

Figure 13.- Time histories of ground force and force-deflection curves for two drops without prerotation where the force-time variation passes through a minimum.

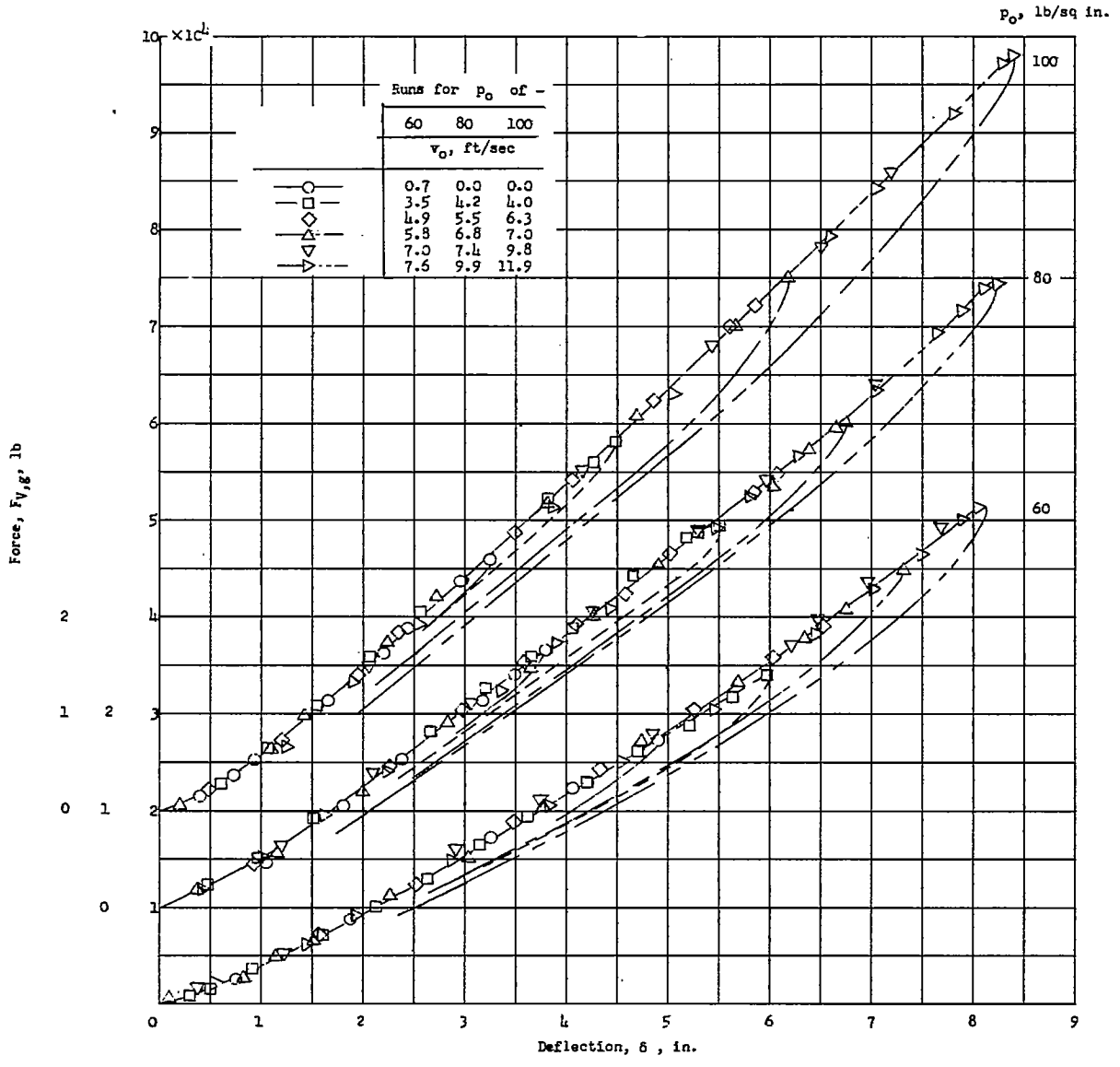

Figure 14.- Variation of vertical ground force with vertical tire deflection obtained from drop tests without prerotation.

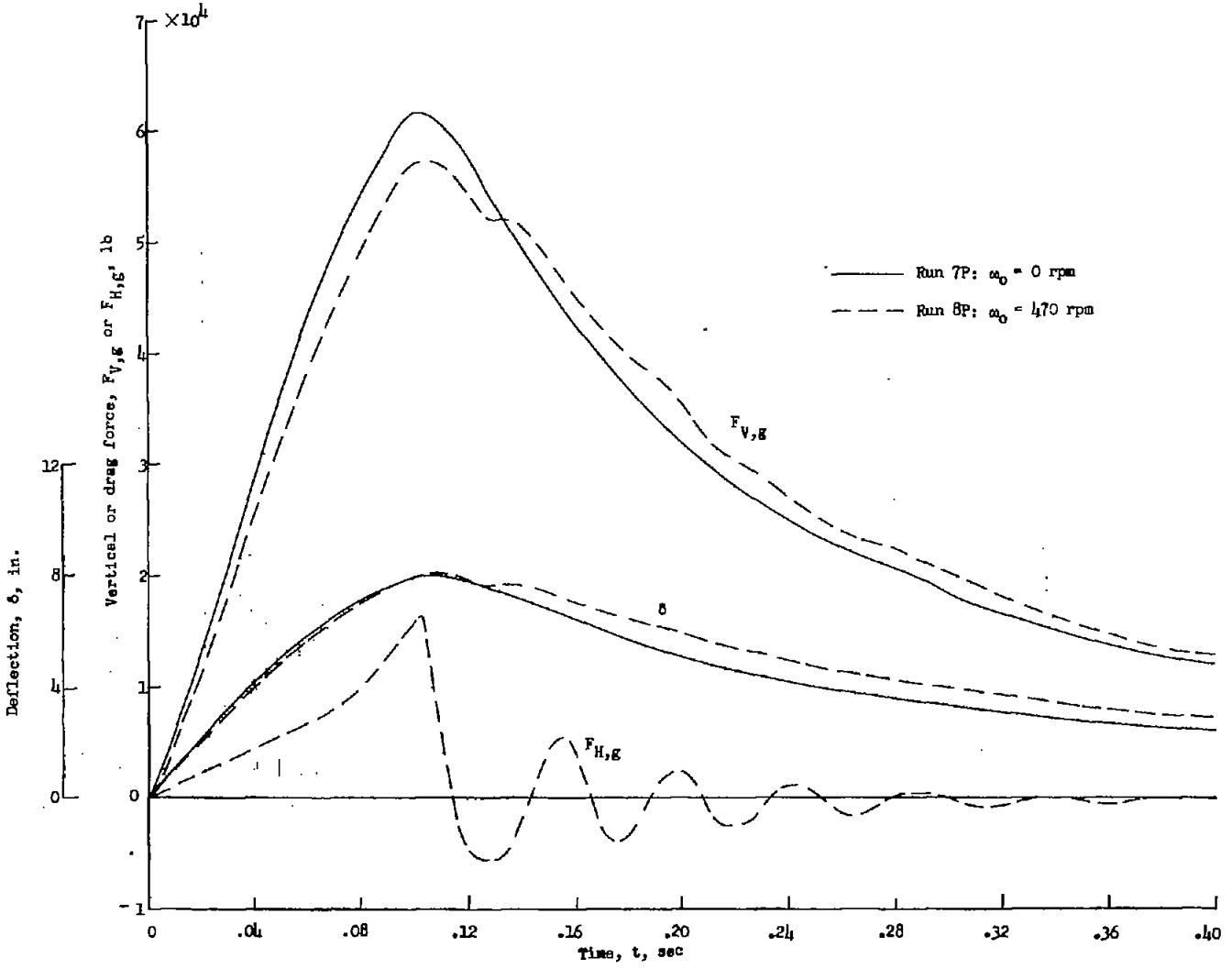

Figure 15.- Time histories of tire ground forces and tire deflection for two drop tests with and without prerotation. $\varphi = 15^{\circ}$; $p_o = 80$ lb/sq in.; $v_o \approx 8.8$ ft/sec.

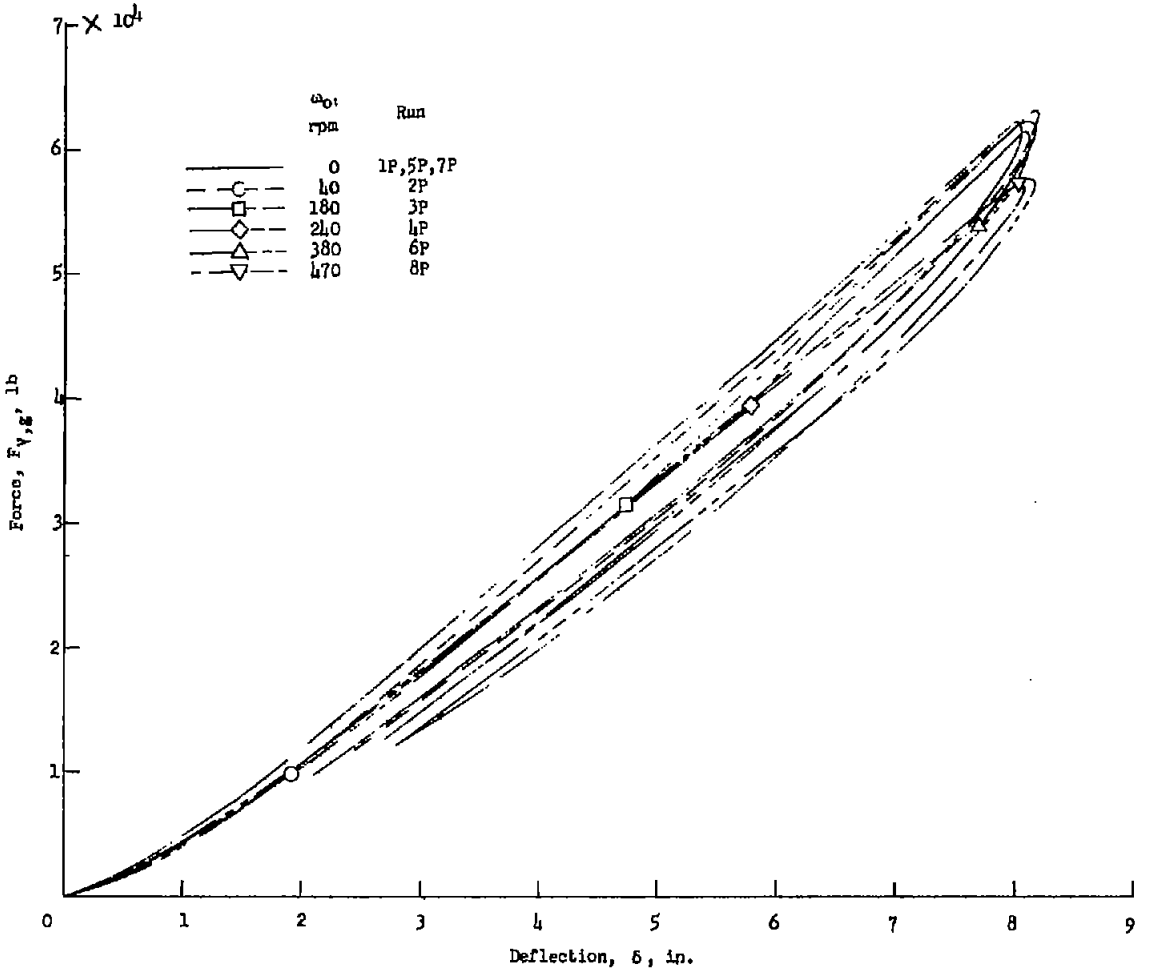

Figure 16.- Variation of vertical ground force with vertical tire deflection obtained from drop tests with prerotation. (The positions of the symbols on the respective curves indicate the force and deflection at which the wheel first reaches zero angular velocity and also maximum drag force.)

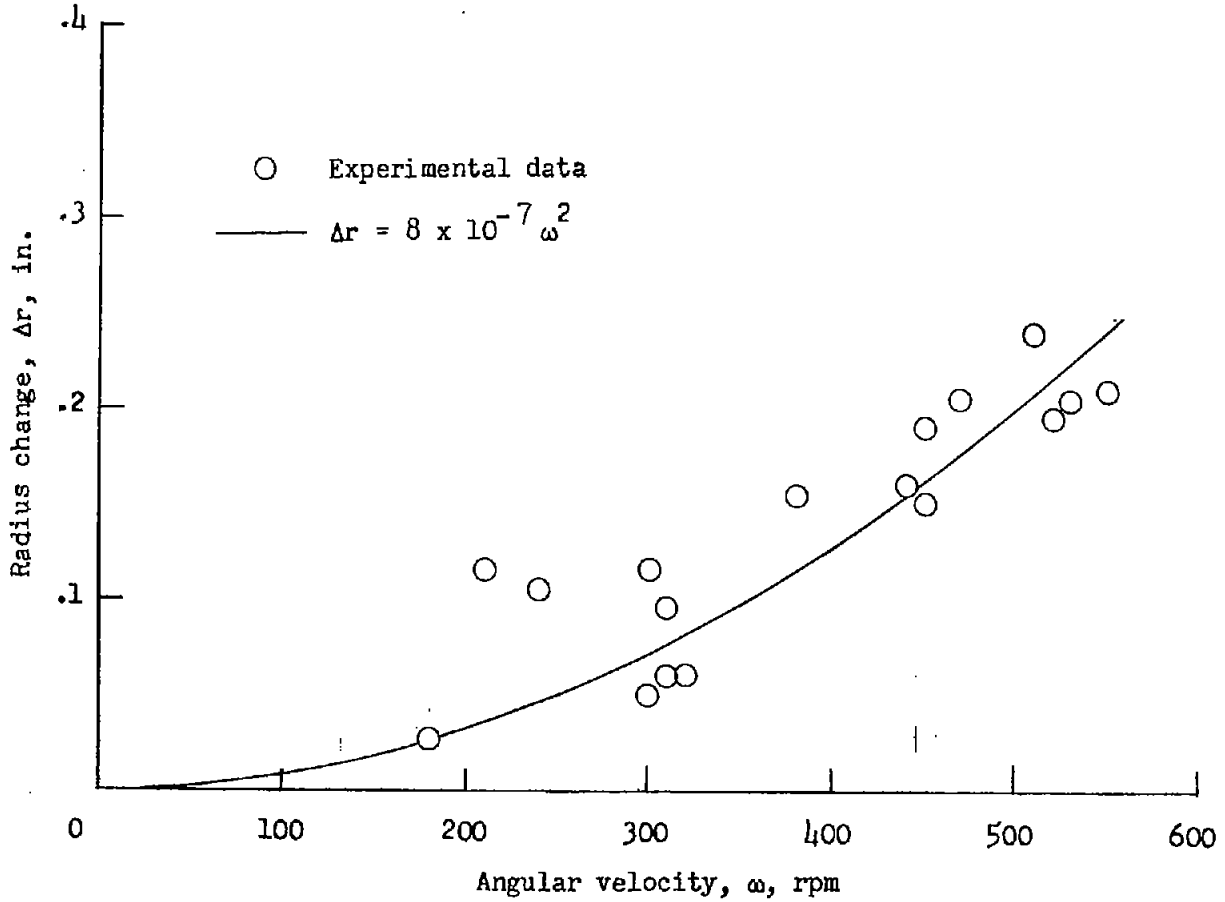

Figure 17.- Variation of tire radius with angular velocity.

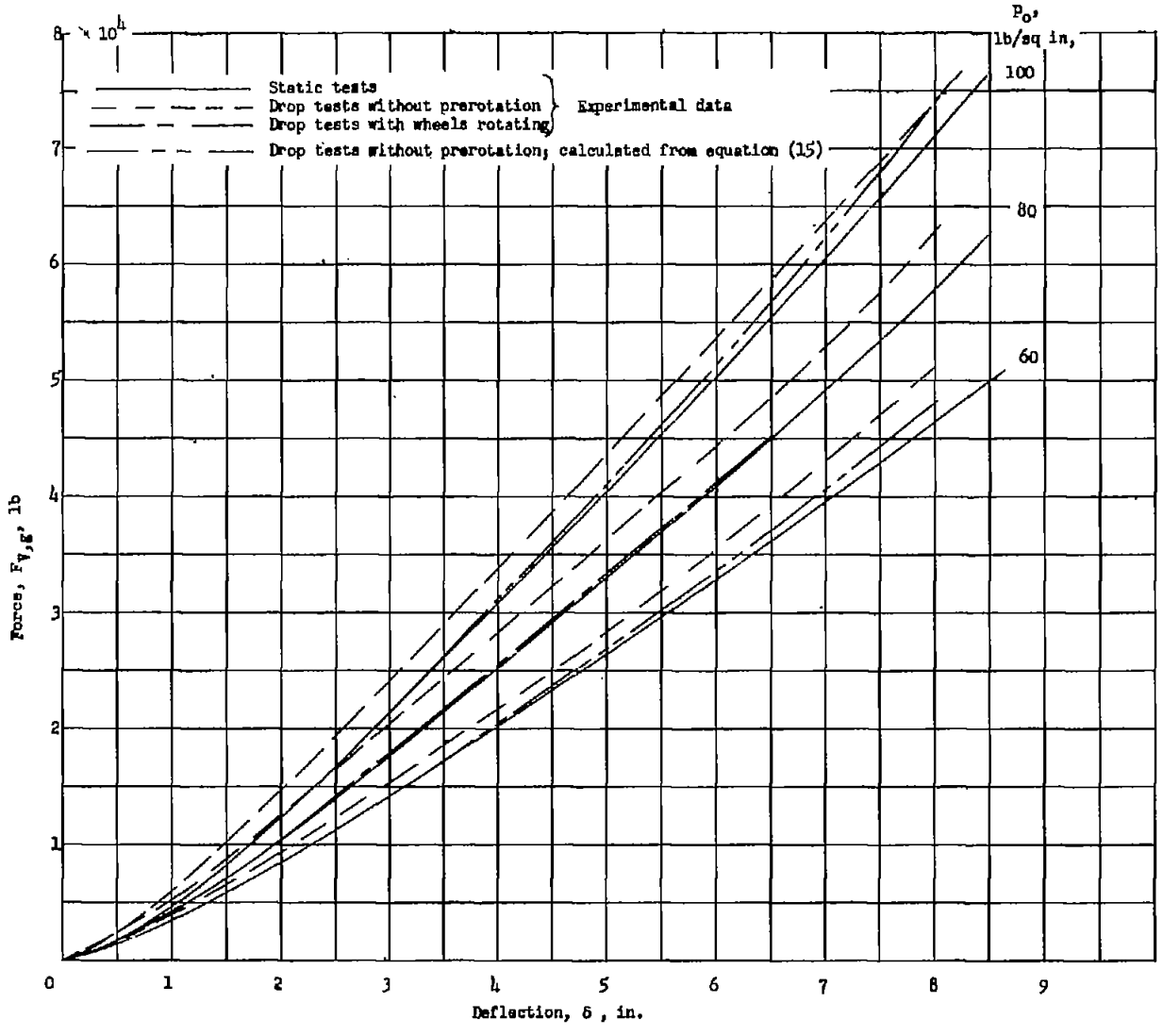

Figure 18.- Comparisons of different types of tire vertical force-deflection characteristics.